Letter

Cosmic string solution to the radio synchrotron background

Bryce Cyr,* Jens Chluba, and Sandeep Kumar Acharya
Jodrell Bank Centre for Astrophysics, School of Physics and Astronomy, The University of Manchester, Manchester M13 9PL, United Kingdom

(Received 13 June 2023; revised 10 November 2023; accepted 7 May 2024; published 4 June 2024)

We investigate the low-frequency spectral emission from a network of superconducting cosmic string loops in hopes of explaining the observed radio synchrotron background. After considering constraints from a variety of astrophysical and cosmological measurements, we identify a best-fit solution with string tension $G\mu \simeq 6.5 \times 10^{-12}$ and current $\mathcal{I} \simeq 2.5 \times 10^{6}$ GeV. This model yields a convincing fit to the data and may be testable in the near future by spectral distortion (TMS, BISOU) and 21 cm experiments (HERA, SKA, REACH). We also find that soft photon heating protects us against current constraints from global 21 cm experiments.

DOI: 10.1103/PhysRevD.109.L121301

Introduction. Over the past decade, radio frequency observations of the sky have received much attention. This has been spurred by two anomalous signals that remain unexplained within ΛCDM. First, the observations of short-duration extragalactic radio pulses dubbed "fast radio bursts" still lack a proven progenitor model [1], though both astrophysical [2] and more exotic models [3–5] have been proposed. Second, the detection of an excess radio background at frequencies $\nu \lesssim 10$ GHz [6,7], often referred to as the "radio synchrotron background" (RSB), still remains unexplained (see Refs. [8,9] for recent reviews). Including the minimal extragalactic background from discrete sources [10], a power-law representation of the RSB is given by

$$T_{\rm RSB}(\nu) \simeq 1.230\ {\rm K}\left(\frac{\nu}{\rm GHz}\right)^{-2.555}. \tag{1}$$

The background surface brightness from known classes of extragalactic point sources appears to be at least a factor of 3 smaller than the observed radio excess [10], with possible explanations having galactic or extragalactic origins [11]. Faint, unresolved/undetected point sources could, in principle, account for the excess; however, in this case the signal is expected to be anisotropic [12]. Current measurements regarding the isotropy of the signal indicate that it may have significantly more angular power on subdegree scales at megahertz frequencies than would be expected from simple point source models [13,14]. Other exotic explanations of the radio excess include synchrotron emission from high-energy particles [15], emission from accreting stellar black holes [16], primordial black holes [17], and others [18]. However, each of these models have their limitations [19] (for example, black hole solutions produce too many UV photons, which leads to stringent constraints from the ionization history [20]), and here we propose a model of superconducting cosmic strings that could explain the anomalous RSB, while being consistent with cosmological and astrophysical datasets.

Cosmic strings are a class of topological defect that may form at the interface of cosmological phase transitions in the very early Universe, provided that the true vacuum manifold of the considered theory is both degenerate and simply connected. If such a phase transition occurs, the Kibble mechanism ensures that a stable network of long strings forms, following a scaling distribution as the Universe expands [21–24]. Further analysis of these models indicates that an abundant distribution of smaller, sub-Hubble string loops may also be sourced through the intersections and self-intersections of long strings in the network. Since these original studies, Nambu-Goto simulations (which neglect the finite thickness of the strings) have been performed, demonstrating the existence [25] of this loop distribution [28–32]. These loops can give rise to a plethora of astrophysical and cosmological signatures, from a stochastic gravitational wave background [33–35] to the seeds of massive black holes [36–38] and more. Gravitational signatures of cosmic strings are typically stronger for phase transitions that take place at higher energy scales. Therefore, cosmic strings represent a well-motivated class of models that help probe aspects of particle physics not accessible by conventional collider

*bryce.cyr@manchester.ac.uk

searches. Their detection (or nondetection) provides us with invaluable glimpses into the nature of the symmetry breaking patterns that the Universe may have undergone at the earliest epochs and highest energies.

It has also been demonstrated that some symmetry breaking patterns can bestow the strings with superconductive properties [39,40]. In these models, $U(1)_{\rm em}$ may be broken in the core of the string, and significant currents can be generated as the loops oscillate and evolve in a background of magnetic fields. These superconducting loops are capable of emitting strong bursts of electromagnetic radiation [41,42], which has led to a variety of constraints on the model space [43–47], most recently in [48]. As a simplifying assumption, the current $\mathcal{I}$ of a superconducting loop distribution is taken to be both time and loop-length independent. In reality, the current is generated dynamically by local magnetic fields, but simulations of this have not been performed and represent an important avenue for future study. As a result, superconducting models are distinguished by two independent parameters, the loop current $\mathcal{I}$ and string tension $G\mu$ (G here is the gravitational constant).

A background of radio photons can be sourced from the incoherent electromagnetic bursts of a network of superconducting string loops. In recent work [48], we considered a variety of constraints on superconducting strings arising from this spectral emission. In particular, we considered the data from ARCADE-2 and other low-frequency experiments measuring the radio background as strict upper limits on the amount of emission allowed by the loop distribution. In this Letter, we now examine the viability of a cosmic string explanation to the observed RSB, showing that there exists an unconstrained region in parameter space that provides a convincing solution.

In the next section, we discuss the mechanism for photon emission from superconducting cosmic strings. Afterward, we briefly review current constraints and provide details about the model that fits well with current observations (see Ref. [48] for more details). Finally, we discuss possible implications and avenues for further study before concluding. Except where stated, we use natural units with $\hbar = c = k = 1$.

Photon production mechanism. At a given initial time $t_{\rm i}$, simulations indicate that most string loops are formed with a length given by some fraction of the Hubble scale, $L_{\rm i} \simeq \beta t_{\rm i}$ where $\beta \simeq \mathcal{O}(0.1)$. Upon formation, the loops undergo oscillations (with period $T \simeq L$), which leads to the formation of substructure on the strings known as cusps and kinks. The substructures decay rapidly once formed, leading to violent bursts of electromagnetic radiation over a wide spectral range if the strings are superconducting. Cusp annihilations typically emit the most energy, and so we neglect the effects of kinks in what follows.

The oscillation-averaged power emitted by a single cusp annihilation is given by $P_\gamma \simeq \Gamma_\gamma \mathcal{I} \mu^{1/2}$, where $\Gamma_\gamma \simeq \mathcal{O}(10)$ is determined by simulations [42,43]. In contrast, the energy carried away by gravitational waves is $P_{\rm g} \simeq \Gamma_{\rm g} G\mu^2$, with $\Gamma_{\rm g} \simeq \mathcal{O}(100)$ [33]. Thus, loops shrink as they emit energy into gravitational and electromagnetic radiation. At any time after formation ($t_{\rm i}$), the loop size is given by

$$L(t) = L_{\rm i}(1+\lambda) - \Gamma G\mu t, \tag{2}$$

where $\Gamma G\mu = (P_{\rm g} + P_\gamma)/\mu$, and $\lambda = \Gamma G\mu/\beta$ is a measure of how quickly after formation a loop will evaporate. Loops with $\lambda \geq 1/\beta$ evaporate within one oscillation time, which can lead to a breakdown of the cusp annihilation formalism described here.

Sufficiently long after the phase transition that formed the strings, a distribution of loops will be established on scales with $L \lesssim \beta t$. The number density of loops per unit length in the matter-dominated era is then given by [32,48]

$$\frac{{\rm d}N_{\rm loops}}{{\rm d}L} \approx \frac{\alpha(1+\lambda)^{3/2} t_{\rm eq}^{1/2}}{t^2 (L + \Gamma G\mu t)^{5/2}} + \frac{\alpha_{\rm m}(1+\lambda)}{t^2 (L + \Gamma G\mu t)^2}. \tag{3}$$

Here, $\alpha = 0.18$ and $\alpha_{\rm m} = \alpha/\sqrt{\beta}$. The first term represents loops forming in the radiation era, while the second is from the larger loops forming during matter domination. A similar form can be found for the evolution in the radiation era, but these are irrelevant for the production of a radio background from loops.

It is evident from Eq. (3) that $L_{\rm c}(t) = \Gamma G\mu t$ defines a special length scale. Indeed, one can show that loops with $L \leq L_{\rm c}(t)$ decay within one Hubble time, so $L_{\rm c}$ acts as the cutoff between a more transient population of decaying loops and the longer-lived set with $L \geq L_{\rm c}(t)$.

The oscillation-averaged photon spectrum produced by a single cusp event (per unit time) is given by [43,48]

$$\frac{{\rm d}^2 E_\gamma^{\rm c}}{{\rm d}\omega {\rm d}t} \simeq \left(\frac{\Gamma_\gamma}{3}\right) \frac{\mathcal{I}^2 L^{1/3}}{\omega^{2/3}}. \tag{4}$$

The spectrum has a high-frequency cutoff at $\omega_{\rm max} \simeq \mu^{3/2}/\mathcal{I}^3 L$, where the produced photons begin to exceed the energy budget allowed by a cusp annihilation.

Using Eq. (4), the full emission spectrum from the loop distribution can be obtained by the appropriately weighted integral,

$$\frac{{\rm d}^2 E_\gamma}{{\rm d}\omega {\rm d}t} = \int_0^{L_{\rm max}} {\rm d}L \, \frac{{\rm d}^2 E_\gamma^{\rm c}}{{\rm d}\omega {\rm d}t} \frac{{\rm d}N_{\rm loops}}{{\rm d}L}, \tag{5}$$

with $L_{\rm max} = \mu^{3/2}/\mathcal{I}^3 \omega$, encoding the fact that only small loops can give rise to arbitrarily high-energy photons (see Ref. [48] for details).

In Fig. 1, we illustrate the evolution of this full spectrum over a range of redshifts for our best-fit string parameters discussed below. The spectrum is well fit by a broken power law, going as $\omega^{-2/3}$ at low frequencies and as $\omega^{-11/6}$

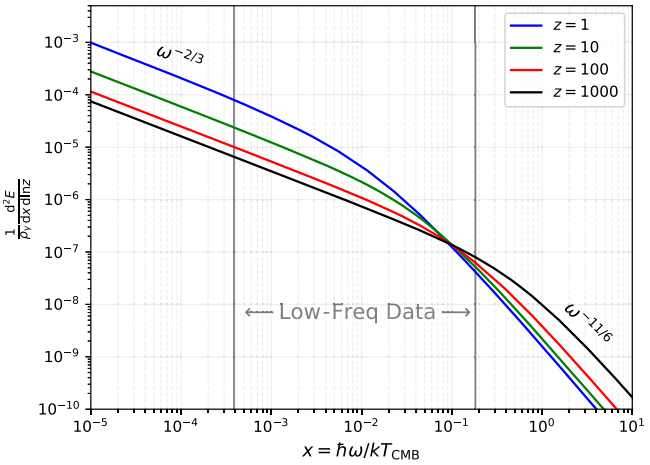

FIG. 1. The instantaneous emission spectrum from a distribution of string loops with $G\mu \simeq 6.5 \times 10^{-12}$ and $\mathcal{I} \simeq 2.5 \times 10^6$ GeV, normalized to the cosmic microwave background (CMB) energy density at each respective redshift. The knee position slowly shifts to lower frequencies at later times. The radio spectrum observed comes from the integrated effect of emission from all loops at all redshifts between the last scattering surface and today.

in the ultraviolet. The position of the knee is determined by the $\omega_{\rm max}$ produced by loops at the cutoff length $L_{\rm c}$. The dropoff in the high-frequency spectrum comes from the fact that these photons are only produced by the short-lived population of loops with $L \lesssim L_{\rm c}(t)$.

A radio synchrotron background from superconducting cosmic strings. In our recent work [48], we considered the constraints on $G\mu$ and $\mathcal{I}$ inferred from the effects of spectral emission by loops on a variety of astrophysical and cosmological phenomena. Specifically, we derived constraints from CMB anisotropies, the optical depth to reionization [49], and spectral distortion data [50]. We furthermore used the radio background data [6,7] and the EDGES observation [51] as upper limits on the model space. In addition, we forecasted constraints from μ, as well as non-μ/non-y–type distortions envisioning a PIXIE-type spectral distortion experiment [52,53]. A summary of these constraints and forecasts (at 2σ) can be found in Fig. 2, which highlights that a wide range in parameter space can already be excluded.

To determine these constraints, we utilized the numerical code CosmoTherm [20,54–57], evaluating the various likelihoods following [48]. However, this time we instead performed a search for possible cosmic string solutions to the anomalous RSB, identifying a region of parameter space capable of fitting the observed radio data at high significance. This region runs along the leftmost edge of the "low-frequency data" contour in Fig. 2. Demanding that we do not violate our other constraints, we find that a distribution of superconducting string loops with $G\mu \simeq 6.5 \times 10^{-12}$ and $\mathcal{I} \simeq 2.5 \times 10^6$ GeV produces a low-frequency radio background that offers a very convincing match to the data.

The left panel of Fig. 3 shows a comparison between our string solution and the best-fit power law we discussed in Eq. (1) ($T_{\rm b} = T_{\rm RSB} + T_{\rm CMB}$). The irreducible background is given by the extragalactic component determined in [10]. We computed the reduced $\Delta\chi^2_{\rm r}$ between an *ad hoc* power-law fit and our strings, finding $\Delta\chi^2_{\rm r} \simeq 0.66$, which indicates an impressive fit to the RSB data [6,7]. The right panel of Fig. 3 shows the raw output from CosmoTherm over an expanded

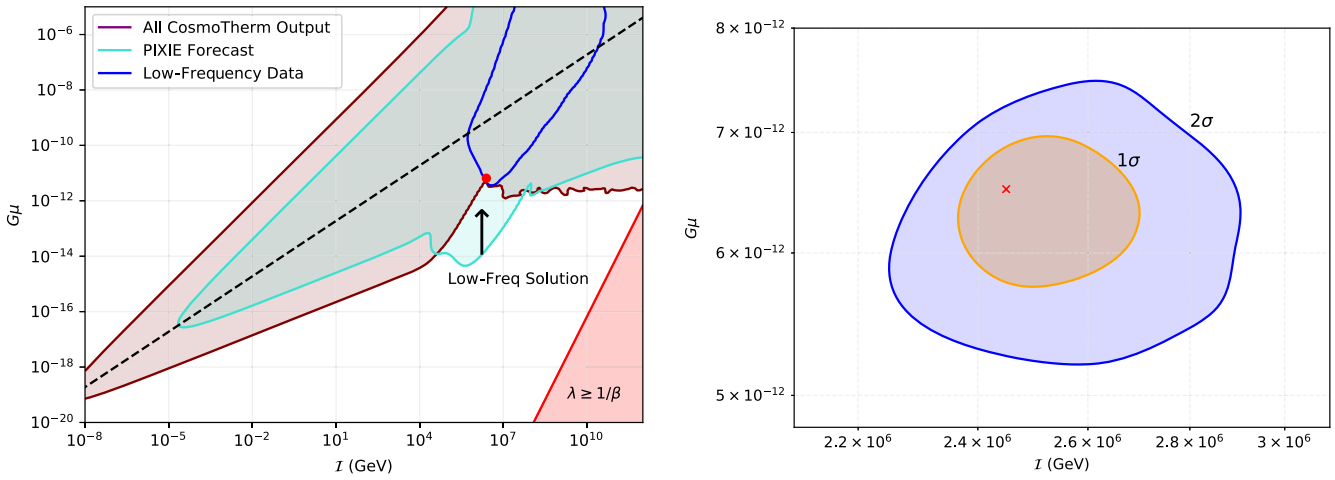

FIG. 2. Left: 2σ constraints from a combined likelihood analysis of a variety of observations [48]. Above the dashed line, gravitational effects determine the lifetime of a loop, while below electromagnetic injection dominates. The red region with $\lambda \geq 1/\beta$ indicates where the oscillation-averaged cusp annihilation formalism breaks down. Right: 1σ (orange) and 2σ (blue) regions around our best-fit solution of $G\mu \simeq 6.5 \times 10^{-12}$ and $\mathcal{I} \simeq 2.5 \times 10^6$ GeV (marked by the red x).

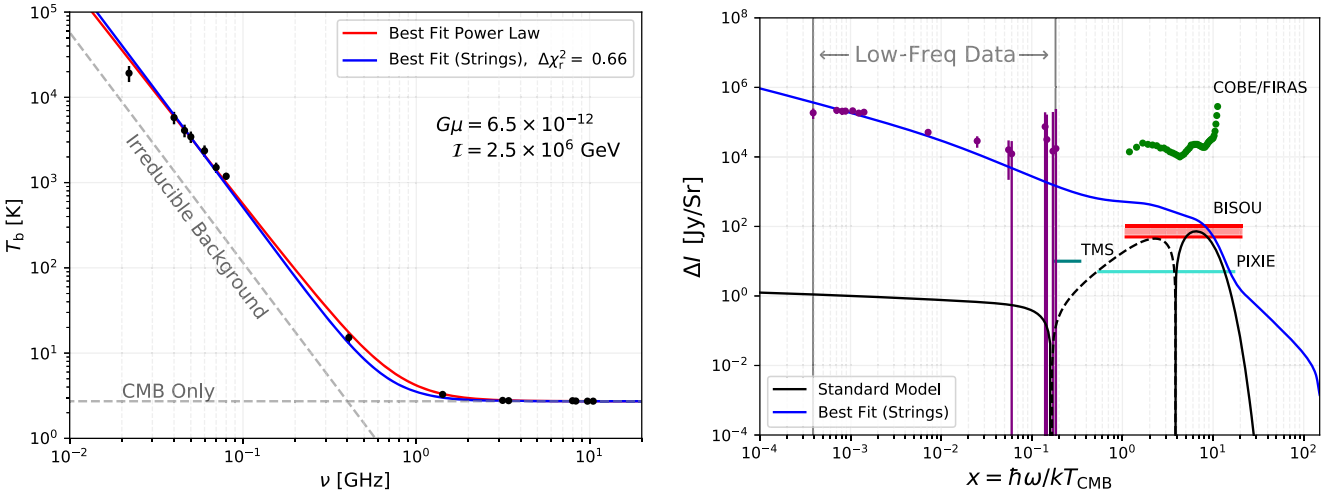

FIG. 3. Left: A comparison of the low-frequency brightness temperature ($T_b = c^2 I/2k\nu^2$) from a best-fit power law (red) and the cosmic string solution (blue). Cosmic strings offer a convincing fit to the radio data [6,7,10]. Right: The raw spectral distortion output from CosmoTherm at $z = 0$. The black line shows the generation of distortions with no strings (reionization effects drive the standard model signal), while the blue line is our string model. The forecasted sensitivities for various experiments indicate that this model can soon be probed at high significance. The tension between the lowest frequency data point and the string model is at the $\simeq 2\sigma$ level.

bandwidth. Note that CosmoTherm determines the spectral distortion ΔI from which the string induced spectrum can be recovered by computing $I_{\rm strings} = I_{\rm BB}(T_{\rm CMB}) + \Delta I$.

We have marked the position of this string solution in both panels of Fig. 2 and find that it lies near the boundary of the constraints derived from CMB anisotropies. The solution ends up being near a contour in parameter space where the knee frequency of the spectrum (see Fig. 1) is $\omega_k \simeq 13.6$ eV at the time of last scattering. This tells us that ionizing photons are not produced efficiently by the string network at that time, which is why CMB anisotropy constraints relax. Without this effect, no RSB solution would be possible.

Another crucial ingredient for the existence of this solution is the inclusion of a newly discovered effect known as "soft photon heating" (SPH) [58], which describes the interplay between extra low-frequency backgrounds and 21 cm observables such as the brightness temperature at cosmic dawn, δT_b. In [58], it was shown that the presence of sufficiently steep low-frequency backgrounds (spectral index $\gtrsim 2.5$ at $\nu \lesssim 1$ GHz) can have a dramatic effect on the absorption depth of δT_b.

It is well known that the amplitude of δT_b is proportional to $T_{\rm rad}/T_{\rm spin}$, where $T_{\rm rad}$ is the brightness temperature of background radiation at the 21 cm wavelength. During cosmic dawn, the dominant contribution to the spin temperature ($T_{\rm spin}$) comes from the kinetic motion of the hydrogen atoms. In Acharya *et al.* [58], we showed that the presence of additional radio backgrounds causes a significant increase in the spin temperature as the hydrogen atoms are heated up. Therefore, SPH generically dampens the amplitude of δT_b.

The EDGES Collaboration has claimed the first detection of the differential brightness temperature at cosmic dawn ($z \simeq 17$) [51]. Before SPH was understood, it was claimed that if the RSB was in place at cosmic dawn, it would produce a δT_b far in excess of what EDGES observed [59]. Importantly, SPH can reconcile these two observations. This is illustrated in Fig. 4, from which it is clear that without the effect we would be in violation of the EDGES bound. The proposed solution therefore represents

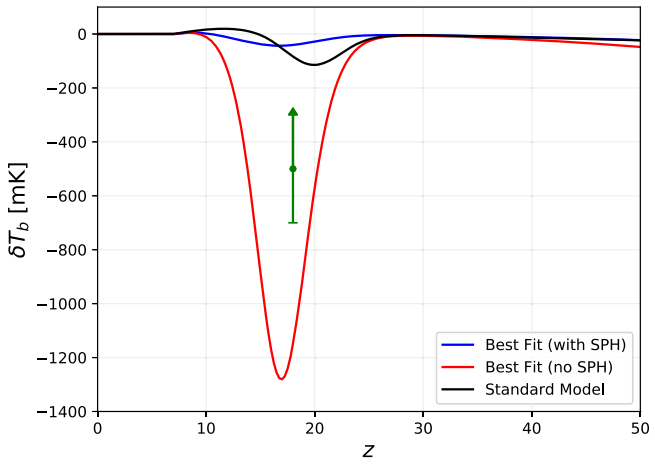

FIG. 4. The differential brightness temperature at cosmic dawn for our best-fit string model with (blue) and without (red) the inclusion of soft photon heating. The EDGES data point is marked in green. Without soft photon heating, this model would be ruled out at more than 2σ by taking EDGES as a strict bound on the amplitude of δT_b.

an important first example of a model that produces a RSB at cosmic dawn, but does not violate global 21 cm observations.

Conclusions. In this work, we have studied the low-frequency spectral signatures produced by a network of superconducting string loops. Using CosmoTherm, we found a region in the $G\mu - \mathcal{I}$ parameter space that offers a convincing explanation to the observed RSB (see Fig. 3). After considering constraints from CMB anisotropies, spectral distortions, the optical depth to reionization, and global 21 cm experiments, we found a best-fit solution to the low-frequency radio data with $G\mu \simeq 6.5 \times 10^{-12}$ and $\mathcal{I} \simeq 2.5 \times 10^{6}$ GeV. This string model is only a marginally worse fit to the data when compared against a completely phenomenological power law ($\Delta\chi^2_r = 0.66$) and offers an intriguing avenue for further study.

While we make no claim that the radio synchrotron background is a smoking-gun signal of superconducting cosmic strings, it is nonetheless intriguing that this model offers such a superb description of the data. The detection of cosmic strings would offer some much-needed insight into the symmetry breaking patterns experienced by our Universe. Thus, we advocate that this simplistic model should be studied in greater detail to fully elucidate its observational signatures.

Superconducting string models are still in need of many refinements. Of particular importance is the simplifying assumption that the current on loops is both time and length independent. Indeed, we know that the current on a loop must be generated dynamically by local magnetic fields and thus is expected to evolve. Using large-scale simulations that study the properties and evolution of $\mathcal{I}$, we could improve our prediction of the RSB from such a network. Additionally, the values of Γ_g and Γ_γ are inferred from simulations and possess an uncertainty that may alter our best-fit values slightly.

Furthermore, our likelihood analysis is simplistic in a number of ways. Most importantly, a proper marginalization over radio foregrounds should be included. In addition, the CMB likelihood can be computed in a more accurate way that might reveal some differences. In the event that only a fraction of the radio background is of extragalactic origin (as hinted at by [60]), the best-fitting contours would move to lower $G\mu$ and $\mathcal{I}$, remaining in unconstrained regions of parameter space. We believe that none of these effects should change the main conclusion drastically.

On the observational frontier, we highlight that the cosmic string solution could be distinguished from a pure power law at $\nu \gtrsim 1$ GHz (see Fig. 3). Current data from ARCADE-2 and FIRAS do not have the required sensitivity, but in the near future TMS [61] is set to improve existing measurements at 10–20 GHz to a sensitivity of 10 Jy/sr. In addition, future measurements with BISOU [62], COSMO [63], and a PIXIE-type experiment [52,53,64] could yield significantly improved limits at $\nu \simeq$ 30–1000 GHz (see Fig. 3), providing an avenue for testing the model. The obtained 21 cm global signal furthermore departs significantly from the standard prediction (see Fig. 4), opening another way to study the cosmic string interpretation, e.g., with REACH [65]. The modified global signal also implies that the 21 cm fluctuations should be significantly altered, identifying a new target for 21 cm cosmology using upcoming experiments such as the SKA [66] and HERA [67,68].

Acknowledgments. This work was supported by the ERC Consolidator Grant CMBSPEC (No. 725456). J. C. was furthermore supported by a Royal Society University Research Fellowship at the University of Manchester, UK (No. URF/R/191023). B. C. would also like to acknowledge support from an NSERC Postdoctoral Fellowship.

[1] J. M. Cordes and S. Chatterjee, Annu. Rev. Astron. Astrophys. **57**, 417 (2019).
[2] B. Zhang, Nature (London) **587**, 45 (2020).
[3] Y.-W. Yu, K.-S. Cheng, G. Shiu, and H. Tye, J. Cosmol. Astropart. Phys. 11 (2014) 040.
[4] J. Ye, K. Wang, and Y.-F. Cai, Eur. Phys. J. C **77**, 720 (2017).
[5] B. Imtiaz, R. Shi, and Y.-F. Cai, Eur. Phys. J. C **80**, 500 (2020).
[6] D. J. Fixsen, Astrophys. J. **707**, 916 (2009).
[7] J. Dowell and G. B. Taylor, Astrophys. J. Lett. **858**, L9 (2018).
[8] J. Singal *et al.*, Publ. Astron. Soc. Pac. **130**, 036001 (2018).
[9] J. Singal *et al.*, Publ. Astron. Soc. Pac. **135**, 036001 (2023).
[10] M. Gervasi, M. Zannoni, A. Tartari, G. Boella, and G. Sironi, Astrophys. J. **688**, 24 (2008).
[11] R. Subrahmanyan and R. Cowsik, Astrophys. J. **776**, 42 (2013).
[12] G. P. Holder, Astrophys. J. **780**, 112 (2014).
[13] A. R. Offringa, J. Singal, S. Heston, S. Horiuchi, and D. M. Lucero, Mon. Not. R. Astron. Soc. **509**, 114 (2021).
[14] F. J. Cowie, A. R. Offringa, B. K. Gehlot, J. Singal, S. Heston, S. Horiuchi, and D. M. Lucero, Mon. Not. R. Astron. Soc. **523**, 5034 (2023).
[15] N. Fornengo, R. Lineros, M. Regis, and M. Taoso, Phys. Rev. Lett. **107**, 271302 (2011).

[16] A. Ewall-Wice, T. C. Chang, J. Lazio, O. Doré, M. Seiffert, and R. A. Monsalve, Astrophys. J. **868**, 63 (2018).
[17] S. Mittal and G. Kulkarni, Mon. Not. R. Astron. Soc. **510**, 4992 (2022).
[18] A. Caputo, H. Liu, S. Mishra-Sharma, M. Pospelov, and J. T. Ruderman, Phys. Rev. D **107**, 123033 (2023).
[19] S. K. Acharya and J. Chluba, Mon. Not. R. Astron. Soc. **521**, 3939 (2023).
[20] S. K. Acharya, J. Dhandha, and J. Chluba, Mon. Not. R. Astron. Soc. **517**, 2454 (2022).
[21] A. Vilenkin and E. P. S. Shellard, *Cosmic Strings and Other Topological Defects* (Cambridge University Press, Cambridge, England, 2000).
[22] T. W. B. Kibble, Phys. Rep. **67**, 183 (1980).
[23] T. W. B. Kibble, J. Phys. A **9**, 1387 (1976).
[24] J. Magueijo and R. H. Brandenberger, in IPM School on Cosmology 1999: Large Scale Structure Formation (2000), arXiv:astro-ph/0002030.
[25] A separate set of field theory simulations that attempt to resolve the cosmic string cores have been performed and do not see a long-lived loop distribution [26,27]. We note that there are significant numerical challenges involved when simulating such a wide range of scales from the string width to the Hubble radius and utilize the loop distributions given from Nambu-Goto simulations in our work.
[26] M. Hindmarsh, S. Stuckey, and N. Bevis, Phys. Rev. D **79**, 123504 (2009).
[27] M. Hindmarsh, J. Lizarraga, J. Urrestilla, D. Daverio, and M. Kunz, Phys. Rev. D **96**, 023525 (2017).
[28] V. Vanchurin, K. D. Olum, and A. Vilenkin, Phys. Rev. D **74**, 063527 (2006).
[29] C. J. A. P. Martins and E. P. S. Shellard, Phys. Rev. D **73**, 043515 (2006).
[30] C. Ringeval, M. Sakellariadou, and F. Bouchet, J. Cosmol. Astropart. Phys. 02 (2007) 023.
[31] L. Lorenz, C. Ringeval, and M. Sakellariadou, J. Cosmol. Astropart. Phys. 10 (2010) 003.
[32] J. J. Blanco-Pillado, K. D. Olum, and B. Shlaer, Phys. Rev. D **89**, 023512 (2014).
[33] T. Vachaspati and A. Vilenkin, Phys. Rev. D **31**, 3052 (1985).
[34] J. Ellis and M. Lewicki, Phys. Rev. Lett. **126**, 041304 (2021).
[35] J. J. Blanco-Pillado, K. D. Olum, and J. M. Wachter, Phys. Rev. D **103**, 103512 (2021).
[36] S. F. Bramberger, R. H. Brandenberger, P. Jreidini, and J. Quintin, J. Cosmol. Astropart. Phys. 06 (2015) 007.
[37] R. Brandenberger, B. Cyr, and H. Jiao, Phys. Rev. D **104**, 123501 (2021).
[38] B. Cyr, H. Jiao, and R. Brandenberger, Mon. Not. R. Astron. Soc. **517**, 2221 (2022).
[39] E. Witten, Nucl. Phys. **B249**, 557 (1985).
[40] J. P. Ostriker, A. C. Thompson, and E. Witten, Phys. Lett. B **180**, 231 (1986).
[41] A. Babul, B. Paczynski, and D. Spergel, Astrophys. J. Lett. **316**, L49 (1987).
[42] A. Vilenkin and T. Vachaspati, Phys. Rev. Lett. **58**, 1041 (1987).
[43] Y.-F. Cai, E. Sabancilar, D. A. Steer, and T. Vachaspati, Phys. Rev. D **86**, 043521 (2012).
[44] H. Tashiro, E. Sabancilar, and T. Vachaspati, Phys. Rev. D **85**, 103522 (2012).
[45] H. Tashiro, E. Sabancilar, and T. Vachaspati, Phys. Rev. D **85**, 123535 (2012).
[46] K. Miyamoto and K. Nakayama, J. Cosmol. Astropart. Phys. 07 (2013) 012.
[47] R. Brandenberger, B. Cyr, and R. Shi, J. Cosmol. Astropart. Phys. 09 (2019) 009.
[48] B. Cyr, J. Chluba, and S. K. Acharya, Mon. Not. R. Astron. Soc. **525**, 2632 (2023).
[49] N. Aghanim *et al.* (Planck Collaboration), Astron. Astrophys. **641**, A6 (2020); **652**, C4(E) (2021).
[50] D. J. Fixsen, E. S. Cheng, J. M. Gales, J. C. Mather, R. A. Shafer, and E. L. Wright, Astrophys. J. **473**, 576 (1996).
[51] J. D. Bowman, A. E. E. Rogers, R. A. Monsalve, T. J. Mozdzen, and N. Mahesh, Nature (London) **555**, 67 (2018).
[52] A. Kogut *et al.*, J. Cosmol. Astropart. Phys. 07 (2011) 025.
[53] A. Kogut, J. Chluba, D. J. Fixsen, S. Meyer, and D. Spergel, Proc. SPIE Int. Soc. Opt. Eng. **9904**, 99040W (2016).
[54] www.Chluba.de/CosmoTherm.
[55] J. Chluba and R. A. Sunyaev, Mon. Not. R. Astron. Soc. **419**, 1294 (2012).
[56] J. Chluba, Mon. Not. R. Astron. Soc. **454**, 4182 (2015).
[57] B. Bolliet, J. Chluba, and R. Battye, Mon. Not. R. Astron. Soc. **507**, 3148 (2021).
[58] S. K. Acharya, B. Cyr, and J. Chluba, Mon. Not. R. Astron. Soc. **523**, 1908 (2023).
[59] C. Feng and G. Holder, Astrophys. J. Lett. **858**, L17 (2018).
[60] N. Fornengo, R. A. Lineros, M. Regis, and M. Taoso, J. Cosmol. Astropart. Phys. 04 (2014) 008.
[61] J. A. Rubiño Martín *et al.*, in *Society of Photo-Optical Instrumentation Engineers (SPIE) Conference Series*, Society of Photo-Optical Instrumentation Engineers (SPIE) Conference Series Vol. 11453 (2020), p. 114530T.
[62] B. Maffei *et al.*, arXiv:2111.00246, 10.1142/9789811269776_0129.
[63] S. Masi *et al.*, arXiv:2110.12254, 10.1142/9789811269776_0131.
[64] J. Chluba *et al.*, Exp. Astron. **51**, 1515 (2021).
[65] E. de Lera Acedo *et al.*, Nat. Astron. **6**, 984 (2022).
[66] https://www.skao.int/.
[67] Z. Abdurashidova *et al.* (HERA Collaboration), Astrophys. J. **925**, 221 (2022).
[68] Z. Abdurashidova *et al.* (HERA Collaboration), Astrophys. J. **924**, 51 (2022).